

A fantastic scenario for ODMR in semiconductors: from spin ensembles to single spins, from boiling helium to boiling water temperatures



Pavel G. Baranov

Ioffe Institute, Saint Petersburg, Russia

“Quantum bits: Better than excellent”

D. DiVincenzo
Nat. Mater, 2010

Modern technology development demands enhanced power efficiency, miniaturization, and speed but these enhancements have their limits. Dominating technology scenarios developed for the semiconductor industry imply that the number of electrons needed to switch a transistor should fall to just one single electron. Any device with nanoscale features inevitably displays some type of quantum behavior and the main task is to exploit quantum-based ideas, to seek a radical technology, with completely novel quantum components operating alongside existing silicon and optical technologies. Spin is a pure quantum object and spin properties begin to play an important and, in some cases, a decisive role in the operation of nanoscale devices. Quantum science seems to transform 21st century technologies.

Electron paramagnetic resonance (EPR) is a tool to manipulate electron spins in solids. Because of the limited sensitivity of conventional EPR, optically detected and electrically detected EPR is favored to detect small numbers of spins. In both approaches, the spin state information

is transferred to a photon or charge state, respectively. In spin-dependent optical emission or photoconductivity, the spin-to-photon or spin-to-charge transfer, respectively, is typically achieved via a spin-dependent recombination process involving paramagnetic states of recombining partners. In optically detected magnetic resonance (ODMR), a microwave-induced repopulation of Zeeman sublevels is detected optically, i.e., there is a giant gain in sensitivity since the energy of an optical quantum is by several orders of magnitude higher than a microwave one. Thus, it becomes possible to detect a very small number of spins down to a single spin! [1, 2].

Until recently, the practical applications of semiconductors involved the use of charge- and spin-carrier ensembles. The capability to efficiently control spin states is the key question of semiconductor spintronics. The unique quantum properties of nitrogen-vacancy (NV) color centers in diamond, which represent a vacancy in the nearest environment of a carbon atom which is replaced by nitrogen [3], have opened a new era in spintronics: it has become possible to manipulate the spin states of a single atomic-size center at room temperature using ODMR. The optical detection of magnetic resonance of a single spin has become possible because of the existence of a unique cycle of optical alignment of the spin sublevel population in the NV center ground state. The prospect of room-temperature quantum information processors now sounds not like science fiction any more. The diamond age of quantum electronics could be just around the corner as has been recently declared by D. D. Awschalom, R. J. Epstein, and R. Hanson, in their article “The Diamond Age of Spintronics”, *Scientific American* 297, 84 (2007).

The unique quantum properties of NV center in diamond have motivated efforts to find defects with similar properties in silicon carbide (SiC), which can extend the functionality of such systems [4–8]. “Quantum bits: Better than excellent” is how D. DiVincenzo titled his article [*Nat. Mater.* 2010]: “excellent” is diamond, “better” is SiC. The NV center, is in many ways the ideal qubit, but diamond is neither cheap nor easily processed into new so-

phisticated devices. There is a Russian proverb “It’s not a tsar’s business”, the diamond-brilliant is too expensive, and not well suited to compete with the existing silicon-based electronics. SiC, which can be regarded as an artificial superlattice, is taking on a new role as a flexible and practical platform for harnessing the new quantum technologies. SiC is a technologically friendly material, used in various devices (LED, MOSFETS, MEMS). A special feature of SiC is the existence of its different polytypes, and for each of the polytypes, the properties of spin color centers are unique; furthermore, even in one polytype, the center may be located in different nonequivalent positions in the lattice. This allows choosing the center with parameters (for instance, optical and microwave ranges) suited for a specific problem. Atomic-scale color centers in bulk and nanocrystalline SiC are considered as a material platform for spintronics, photonics compatible with fiber optics, quantum information processing and sensing at ambient conditions. Their spin state can be initialized, manipulated and read out by means of ODMR, via level anticrossing (LAC) and cross-relaxation (CR) [9–19]. A convincing point with SiC is that, similar to diamond, the stable spinless nuclear isotopes guarantee long dephasing times. Finally, coherent manipulation of spin states has been performed at room temperature and even at temperatures higher than room temperature by hundreds of degrees. It has been shown that there are at least two families of color centers in SiC with $S = 1$ and $S = 3/2$, which have the property of optical alignment of the spin levels and allow a spin manipulation. The spin-1 center is a SiC divacancy of the neighboring positions with covalent molecular bond. The spin-3/2 center is a negatively charged silicon vacancy V_{Si}^- in the paramagnetic state, that is noncovalently bonded to the neutral carbon vacancy V_C^0 in the non-paramagnetic state, located on the adjacent site along the SiC symmetry c axis. These centers are usually referred to as the corresponding zero-phonon lines (ZFLs). For the $S = 3/2$ family, the ground state and the excited state were demonstrated to have spin $S = 3/2$ and a population inversion in the ground state can be generated using opti-

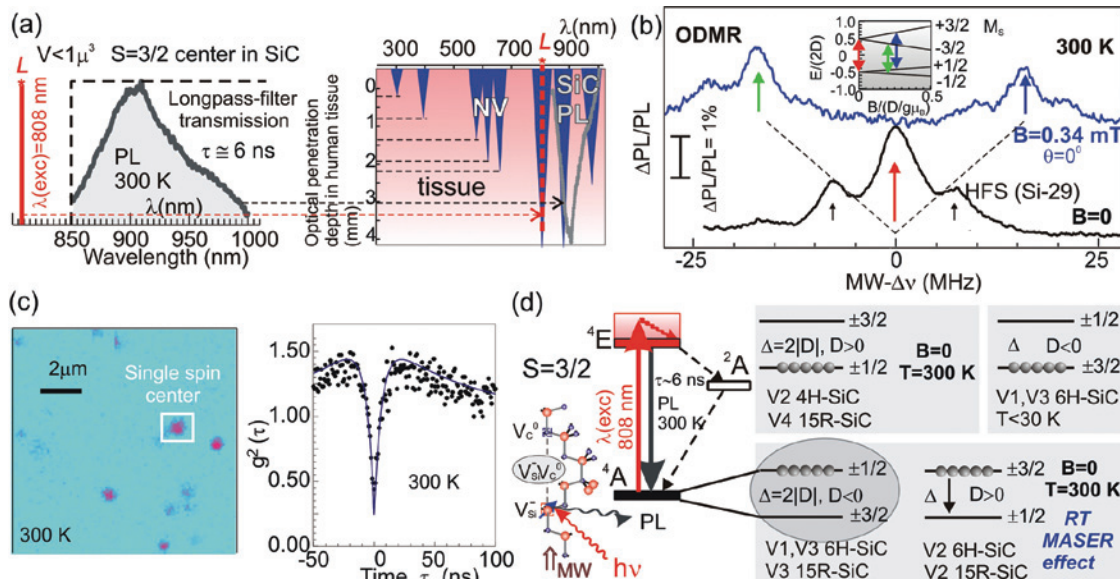


Fig. 1. a) An example of the room temperature photoluminescence (PL) spectra of spin-3/2 centers in SiC (left); the depth of light penetration (in the form of blue peaks) into biological tissues for different wavelengths of light (right). b) A typical ODMR signal of the spin-3/2 centers in SiC in zero and $B = 0.34$ mT magnetic fields. A hyperfine structure (HFS) with twelve Si atoms of the next nearest-neighbor (NNN) shell is shown. c) Confocal raster scan of single color center photoluminescence (PL) in SiC and a correlation function of the color center. d) The schemes of optically induced alignment of spin level populations for spin-3/2 centers and possible configurations of spin-3/2 center. For more information see ref. [20].

cal pumping, leading to stimulated microwave emission even at room temperature and above.

Spin-1 and spin-3/2 centers in SiC emit in the near-IR, that is, in the vicinity of fiber-optic transparency band. As a result, one could do quantum manipulation at room temperature in the materials which are used for electronics at telecommunications frequencies. Jörg Wrachtrup, who pioneered the manipulation of single-defect spin states in diamond [3], sees potential applications for SiC defects beyond quantum computing [see *Physics Today*, 2011]. “I could envision using tiny silicon carbide crystals to do micro- or nanoscale magnetic resonance imaging on cells and other biological systems. It really could open up a whole new world of scientific applications”.

In line with this statement, Figure 1a shows an example of the room temperature photoluminescence (PL) spectra of spin-3/2 centers in SiC. The right-hand picture shows the depth of light penetration into biological tissues for different wavelengths of light. It can be seen that the spectral range for centres in SiC is more favorable compared to the optical characteristics of NV centres in diamond according to K. Kalka, H. Merk, H. Mukhtar (*J. Am. Acad. Dermatol.* 42, 389, 2000).

Figure 1b presents a typical experimental microwave (MW) dependence of the ODMR signal of the spin-3/2 centers in SiC, $\Delta\nu$ is the zero-field splitting (ZFS). The ODMR signal is detected under laser excitation $\lambda = 808$ nm

in zero and $B = 0.34$ mT magnetic fields. The vertical bar indicates the ODMR contrast. A hyperfine structure (HFS) due to the interaction with ^{29}Si nuclei for twelve Si atoms in the next nearest-neighbour (NNN) shell of the Si vacancy is shown by arrows. The inset shows the energy level diagram and corresponding resonance transitions. Figure 1c shows a confocal raster scan of the single-colour center PL at 300 K in 4H-SiC; bright spots indicate V2 emitters (left) and the right hand picture shows the intensity time correlation function of colour center in the square, showing photon antibunching at zero delay, proving that the studied colour center is a single one. The schemes of optically induced alignment of spin level populations in a zero magnetic field at room temperature for spin-3/2 centers (possible configuration is depicted) in different SiC polytypes are shown in Fig. 1d.

Figure 2a, as an example, shows signals of room temperature ODMR and level anti-crossing (LAC) of the V2 spin centers in a 4H-SiC crystal. The signals were recorded by lock-in detection of the change in the PL in the near-IR range with application of a constant magnetic field and an oscillating low-frequency magnetic field. The energy of the corresponding spin levels is shown at the top. The LAC in the absence of the MW field (MW “off”), denoted as LAC1 and LAC2; for LAC1 $B = D$ and for LAC2 $B = 2D$, where ZFS $\Delta = 2|D|$, and two ODMR signals recorded at

the MW field on 40 and 45 MHz are shown. The choice of frequencies was due to the fact that when the ODMR signal approaches the LAC1 signal, the ODMR signal increases several times and approaches the LAC1 signal intensity. The ODMR line shift ΔB at frequencies of 40 and 45 MHz is shown demonstrating the principle of measuring magnetic fields by the ODMR method. The point of the LAC1 weakly depends on the orientation of the crystal in a magnetic field, and therefore it can be used for measuring magnetic fields (and temperatures with LAC1 for excited state) in powder materials. It is assumed that if

the ODMR signal coincides with the LAC, polarization of the surrounding silicon ^{29}Si and ^{13}C carbon nuclei with long relaxation times is possible through hyperfine interactions. Circles indicate areas of reduction of the signals with a certain polarization of ^{29}Si , which are present in the signals of the ODMR in the form of satellites. We assume that optical registration of nuclear magnetic resonance on polarized nuclei ^{29}Si and ^{13}C of spin centers in SiC will find a number applications (quantum computing, NMR imaging, gyroscopes, etc). In Fig. 2b the PL zero-phonon lines (ZPLs) in 15R-SiC of the corresponding spin-3/2 centers (top) and X-band direct-detected (DD) EPR spectra induced with ZFLs V2, V3 and V4 (bottom) are demonstrated. In Fig. 2c (bottom) optically induced ESE spectra measured in 15R-SiC are shown; the light-induced inverse population of the spin sublevels of V2 centers is depicted in the inset. Figure 2c (top) shows the ENDOR spectra measured for the low field (lf) and high-field (hf) transitions indicated in the ESE spectra [16].

Observed Rabi nutations in SiC persist for about 0.1 ms at RT and there is evidence that the probed spin ensemble can be prepared in a coherent superposition of the spin states. The electron spin of the spin-3/2 centers can be manipulated by a low-energy microwave field of 1–300 MHz which is compatible with NMR imaging. The color centers in SiC are optically active in the near infrared spectral

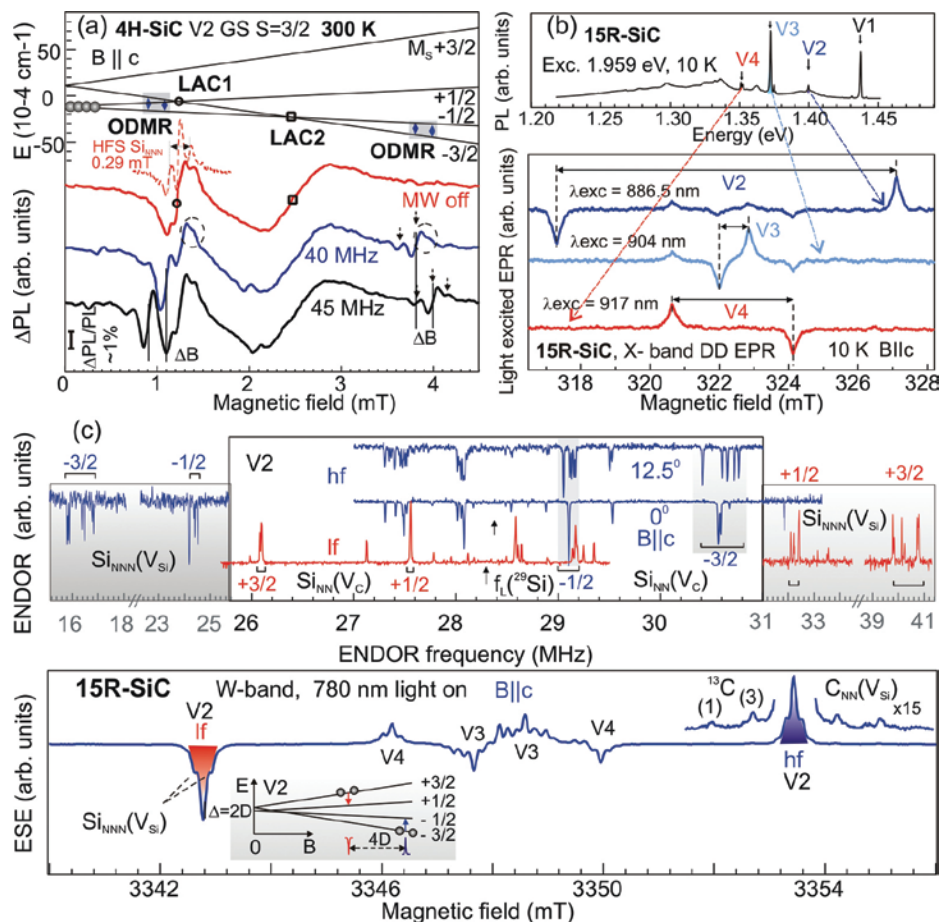


Fig. 2. a) Room-temperature detection of the change in PL of spin-3/2 centers in a 4H-SiC: the level anti-crossing (LAC) signals (MW off) and ODMR. ODMR line shift ΔB in a magnetic field for two frequencies demonstrates the principle of measuring magnetic fields (DD). b) (top) The PL ZPLs in 15R-SiC of the corresponding spin-3/2 centers. (bottom) X-band direct-detected (DD) EPR spectra induced with ZFLs V2, V3 and V4. (c) (bottom) Optically induced ESE spectra measured in 15R-SiC. (top) ENDOR spectra measured for the lf and hf transitions indicated in the ESE spectra. For more information see ref. [16].

region, which is preferential for potential in vivo biological applications due to the deepest tissue penetration and which is compatible with fiber optics. The concept of sensing is based on variants of the ODMR technique with sensitivity down to a single-spin [4, 13, 14]. Demonstrated spin properties of the color centers in SiC and related nanostructures open up new avenues for quantum computing, quantum sensing, bio-labeling, for future single-particle and single defect quantum devices and related biomedical sensors. The optically induced population inversion of spin states at RT leads to stimulated microwave emission, which can be used to implement solid-state masers and extraordinarily sensitive radiofrequency amplifiers.

Quantum technologies based on coherent control of the spins of color centers in diamond and silicon carbide have developed fantastically over the past two decades. The combination of supersensitive optical techniques for high-resolution image detection and reliable coher-

ent control using magnetic resonance are key components in the development of the first quantum devices based on these materials. The possibility of highly accurate scaling of color centers and achieving long coherence times opens up new prospects for so-called hybrid quantum processes, in which color centers are associated with different types of qubits. There is no doubt that this area of research will develop rapidly in the near future and, as can be expected, will lead to the emergence of new quantum technologies.

Support by the Russian Science Foundation (RSF) was extremely important in writing the Springer book “Magnetic Resonance of Semiconductors and Their Nanostructures: Basic and Advanced Applications” [4]. We would like to thank K. M. Salikhov and L. V. Mosina for the offer to write this book. It became possible to carry out a number of works on spin centers in SiC with financial support from the RSF, Project No. 20-12-00216.

References

1. J. Köhler, J. A. J. M. Disselhorst, M. C. J. M. Donckers, E. J. J. Groenen, J. Schmidt, W. E. Moerner, *Nature* 1993, 363, 242–244.
2. J. Wrachtrup, C. von Borczyskowski, J. Bernard, M. Orrit, R. Brown, *Nature* 1993, 363, 244–245.
3. A. Gruber, A. Dräbenstedt, C. Tietz, L. Fleury, J. Wrachtrup, C. von Borczyskowski, *Science* 1997, 276, 2012–2014.
4. P. G. Baranov, H.-J. von Bardeleben, F. Jelezko, J. Wrachtrup, *Magnetic Resonance of Semiconductors and Their Nanostructures: Basic and Advanced Applications*: Springer Series in Materials Science, Volume 253, 2017.
5. P. G. Baranov, I. V. Il'in, E. N. Mokhov, M. V. Muzafarova, S. B. Orlinskii, J. Schmidt, *JETP Lett.* 2005, 82, 441.
6. P. G. Baranov, A. P. Bundakova, I. V. Borovykh, S. B. Orlinskii, R. Zondervan, J. Schmidt, *JETP Lett.* 2007, 86, 202.
7. J. R. Weber, W. F. Koehl, J. B. Varley, A. Janotti, B. B. Buckley, C. G. Van de Walle, D. D. Awschalom, *Proc. Natl. Acad. Sci.* 2010, 107, 8513.
8. P. G. Baranov, A. P. Bundakova, A. A. Soltamova, S. B. Orlinskii, I. V. Borovykh, R. Zondervan, R. Verberk, J. Schmidt, *Phys. Rev. B* 2011, 83, 125203.
9. D. Riedel, F. Fuchs, H. Kraus, S. Vath, A. Sperlich, V. Dyakonov, A. Soltamova, P. Baranov, V. Ilyin, G. V. Astakhov, *Phys. Rev. Lett.* 2012, 109, 226402.
10. H. Kraus, V. A. Soltamov, F. Fuchs, D. Simin, A. Sperlich, P. G. Baranov, G. V. Astakhov, V. Dyakonov, *Scientific Reports* 2014, 4, 5303.
11. H. Kraus, V. A. Soltamov, D. Riedel, S. Vath, F. Fuchs, A. Sperlich, P. G. Baranov, V. Dyakonov, G. V. Astakhov, *Nature Phys.* 2014, 10, 157.
12. D. Simin, V. A. Soltamov, A. V. Poshakinskiy, A. N. Anisimov, R. A. Babunts, D. O. Tolmachev, E. N. Mokhov, M. Trupke, S. A. Tarasenko, A. Sperlich, P. G. Baranov, V. Dyakonov, G. V. Astakhov, *Phys. Rev. X* 2016, 6, 031014.
13. M. Widmann, S.-Y. Lee, T. Rendler, N. T. Son, H. Fedder, S. Paik, L.-P. Yang, N. Zhao, S. Yang, I. Booker, A. Denisenko, M. Jamali, S. Ali Momenzadeh, I. Gerhardt, T. Ohshima, A. Gali, E. Janzén, J. Wrachtrup, *Nature Materials* 2015, 14, 164.
14. D. J. Christle, A. L. Falk, P. Andrich, P. V. Klimov, J. U. Hassan, N. T. Son, E. Janzén, T. Ohshima, D. D. Awschalom, *Nature Materials* 2015, 14, 160.
15. A. N. Anisimov, D. Simin, V. A. Soltamov, S. P. Lebedev, P. G. Baranov, G. V. Astakhov, V. Dyakonov, *Scientific Reports* 2016, 6, 33301.
16. V. A. Soltamov, B. V. Yavkin, D. O. Tolmachev, R. A. Babunts, A. G. Badalyan, V. Yu. Davydov, E. N. Mokhov, I. I. Proskuryakov, S. B. Orlinskii, P. G. Baranov, *Phys. Rev. Lett.* 2015, 115, 247602.
17. S. A. Tarasenko, A. V. Poshakinskiy, D. Simin, V. A. Soltamov, E. N. Mokhov, P. G. Baranov, V. Dyakonov, G. V. Astakhov, *Phys. Status Solidi B* 2018, 255, 1700258 (1 of 9).
18. T. Ohshima, T. Satoh, H. Kraus, G. V. Astakhov, V. Dyakonov, P. G. Baranov, *TOPICAL REVIEW*, *J. Phys. D: Appl. Phys.* 2018, 51, 333002 (1–14).
19. V. A. Soltamov, C. Kasper, A. V. Poshakinskiy, A. N. Anisimov, E. N. Mokhov, A. Sperlich, S. A. Tarasenko, P. G. Baranov, G. V. Astakhov, V. Dyakonov, *Nature Communications*, 2019, 10:1678 <https://doi.org/10.1038/s41467-019-09429-z>
20. P. G. Baranov, A. M. Kalashnikova, V. I. Kozub, V. L. Korenev, Yu. G. Kusrayev, R. V. Pisarev, V. F. Saepa, I. A. Akimov, M. Bayer, A. V. Scherbakov, D. R. Yakovlev, *Physics – Uspekhi* 2019, 62(8), 795–822.